Soft Matter

The contribution of network elasticity to electro-optic response in polymer stabilized cholesteric liquid crystals

Journal:	*Soft Matter*
Manuscript ID	SM-ART-02-2023-000225.R1
Article Type:	Paper
Date Submitted by the Author:	21-Apr-2023
Complete List of Authors:	Radka, Brian; University of Colorado, Chemical and Biological Engineering Pande, Gaurav; University of Colorado, Chemical and Biological Engineering White, Tim; University of Colorado, Chemical and Biological Engineering

ARTICLE

The contribution of network elasticity to electro-optic response in polymer stabilized cholesteric liquid crystals

Received 00th January 20xx,
Accepted 00th January 20xx

DOI: 10.1039/x0xx00000x

Brian P. Radka,[a] Gaurav K. Pande,[a] Timothy J. White*[a]

Polymer stabilization of cholesteric liquid crystals can enable dynamic reconfiguration of the selective reflection of the CLC phase. Here, we explore how the contribution of the elasticity of the polymer stabilizing network affects the ion-mediated, electromechanical deformation and associated electro-optic response in PSCLCs. We utilize a free-radical chain transfer reaction between acrylate and thiol monomers that has been used to prepare elastomeric networks. This work maps the compositional contributions of total concentration and crosslink density to tuning and recovery

Introduction

Composites prepared from polymers and liquid crystals (LCs) enable distinctive electro-optic behaviors. A subset of polymer/LC composites are polymer stabilized cholesteric liquid crystal (PSCLCs). PSCLCs integrate small concentrations of polymer to stabilize the inherent reflection of the cholesteric liquid crystal (CLC) phase. Polymer stabilization distinctly enables dynamic and reversible electrical manipulation of optical properties in the CLC phase.[1–3]

In the planar orientation, the CLC phase is inherently reflective due to the periodic rotation of the LC director across the thickness. This is illustrated in Fig. 1a with the blue ellipses representing the LC mesogens. The periodicity of the phase is characterized by the distance over which the director rotates 360°, called the pitch length (P). The pitch length is easily adjusted by the concentration of the chiral dopant mixed with a nematic LC.[4] Due to the periodic and helical nature of the CLC phase, the selective reflection is circularly polarized at the wavelength of light is approximately equal to the pitch length. The handedness of the reflection matches the handedness of the CLC. The reflection at normal incidence is defined by the center of the reflection notch ($\lambda_c = n_{avg} \times P$) and the bandwidth of the reflection ($\Delta\lambda = \Delta n \times P$) where n_{avg} is the average of extraordinary (n_e) and ordinary (n_o) refractive indexes and Δn is their difference.[5–7]

Polymer stabilization is a facile route to realize electro-optic response not achievable in low molar mass CLC system.[8–10] The polymerization of crosslinkable monomer (typically 3-10wt%) in a CLC creates a bicontinuous phase characterized by polymer fibrils interspersed with the low molar mass CLC. The polymer fibrils retain "structural chirality", that matches the handedness of the CLC phase, this is represented in Fig. 1a with the black lines. [2,11] Typically, the monomers selected for polymer stabilization are liquid crystalline to assist with solubility and avoid phase separation, however, LC monomers are not required.[12] The stabilization occurs by virtue of the polymer network interfacing with the low molar mass LC host. In some sense, the polymer stabilizing network can be thought of as a through-thickness anchoring layer.[13] The influence of the polymer/LC interaction is evident in the increase in the isotropic transition temperature when the polymer network is introduced.[14]

Early studies explored reflection switching in PSCLCs prepared with positive dielectric anisotropy ($\Delta\varepsilon > 0$) liquid crystals. Upon application of the field above a threshold voltage the low molar mass liquid crystal aligns parallel to the field direction into the clear homeotropic state. After removal of the field, the polymer stabilizing network expedites the reformation of the CLC phase and avoids the formation of metastable focal conic states because the CLC takes on the local orientation of the polymer network.[9,13] More recently, dynamic reconfiguration of the reflection has been explored in PSCLCs formulated with a negative dielectric anisotropy ($\Delta\varepsilon < 0$) host. Upon application of a field, the host does not reorient and retains the reflective properties. Phenomenologically, depending on the material choice and processing conditions, various dynamic and reversible electro-optic responses have been observed including bandwidth broadening, notch splitting, red-shifting tuning, and blue-shifting tuning.[15–22]

The proposed mechanism for the dynamic response of PSCLCs with $\Delta\varepsilon < 0$ is thought to be the result of the deformation of the structurally chiral polymer network to an applied DC field. The electromechanical coupling is hypothesized to be associated with cations trapped on or within the polymer network.[17,19,21,23–25] When a sufficiently strong electric field has been applied, the charged species impart a mechanical force on the polymer network,

[a] Department of Chemical and Biological Engineering, University of Colorado, Boulder, CO 80309, USA.
E-mail: Timothy.J.White@colorado.edu

Electronic Supplementary Information (ESI) available: [details of any supplementary information available should be included here]. See DOI: 10.1039/x0xx00000x

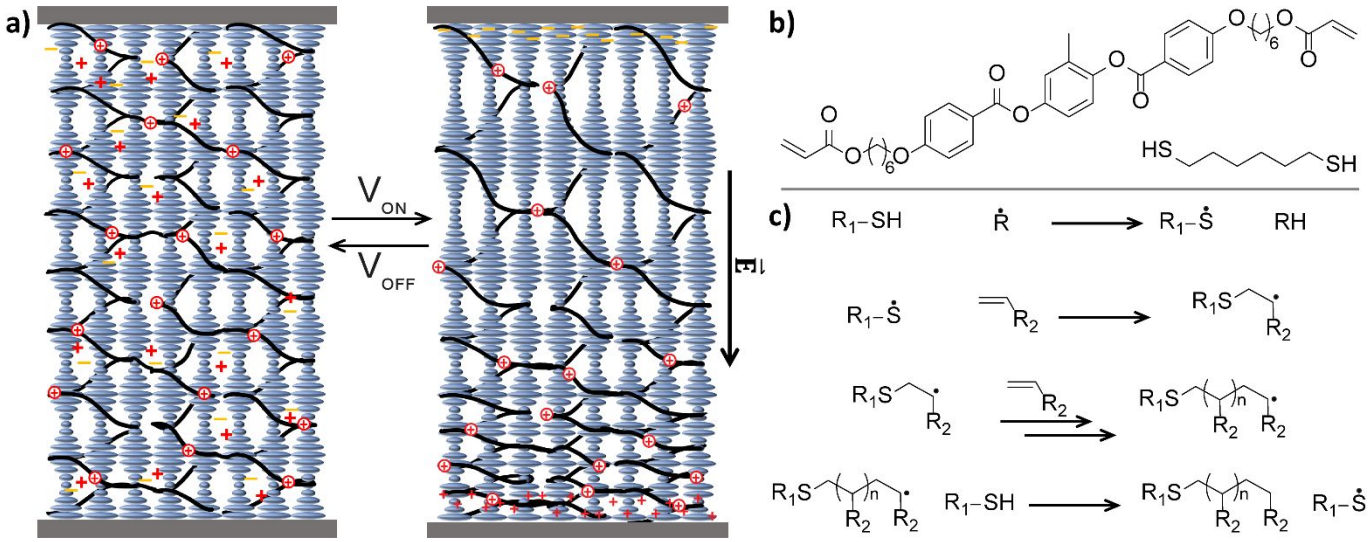

Fig. 1 (a) An illustrative example of the dynamic electro-optic tuning in PSCLC devices. The blue ellipsoids represent the CLC host, the black lines the polymer network, + and – the free ionic species, and ⊕ the trapped cations. (b) The molecular structures of the monomers used in this study, liquid crystalline RM82 and hexane dithiol. (c) The mechanism for free radical polymerization of a thiol/acrylate system. From top to bottom the reactions are the radical initiation of the thiol monomer, thiol acrylate polymerization, acrylate homopolymerization, and thiol chain transfer.

deforming it in plane with the electric field. This distortion results in a heterogenous pitch length, where the PSCLC has regions of expanded and contracted pitch length. The ion-mediated mechanism is indirectly informed in that the region closer to the cathode has an expanded pitch length and the region closer to the anode has a contracted pitch length. Again, the CLC host takes on the local chirality of the polymer stabilizing network, due to anchoring. The depth dependent pitch length that develops upon application of an electric field results in a myriad of optical responses informed by the distribution of the pitch. Upon the release of the voltage, the elastic nature of the polymer network returns the polymer network and pitch length to the original state, as illustrated in Fig. 1a.

Historically, the stabilizing network in PSCLCs have been prepared by photoinitiated polymerization of liquid crystalline diacrylate monomers. In many of these prior reports, the elasticity of the polymer network is realized by utilizing a high initiator to monomer ratio to decrease the kinetic chain length during polymerization.[26] Here, we expand upon these prior studies in exploring the effect of elasticity on the electro-optic response of PSCLCs. Specifically, we explore the use of thiol-acrylate copolymerization with a linear dithiol, a reaction commonly used to reduce the crosslink density of liquid crystal elastomers.[27–30]

Results and Discussion

The polymer stabilizing network is formed through a free-radical chain transfer reaction[31] via the copolymerization of the liquid crystalline diacrylate monomer RM82 and hexane dithiol (HDT) (Fig. 1b). The inclusion of the dithiol reduces the crosslink density of the polymer stabilizing network via both chain extension and chain transfer. Chain extension occurs when both thiol groups in HDT react with an acrylate group, by inserting a linear unit between the acrylate groups rather than allowing them to react directly the average distance between crosslinks is increased. Chain transfer occurs when a propagating polymer chain transfers the radical reactivity to an unreacted thiol group. The deactivated polymer chain is now non-reactive and a dangling end in the polymer network, the thiol radical can now start the prorogation of another chain. These potential reaction pathways are illustrated in Fig. 1c.

NMR measurements of the non-reacted components of a model polymer stabilized nematic liquid crystal, which were extracted post polymerization and compared to the mixture before polymerization, shows no discernible concentration of either monomer (Fig. S1d). This confirms that the dithiol monomer is nearly completely incorporated into the polymer network in some manner. FTIR measurements on the unreacted mixture as well as the isolated polymer network (Fig. S2) were also examined. Unfortunately, due to the weak signal and low concentration of thiols it is not possible to quantify the degree of thiol conversion nor the ratio of chain extension to chain transfer. However, FTIR examination corroborates the incorporation of thiol into the polymer stabilizing network with the significant reduction in the thiol signal at 2573 cm^{-1} between the unreacted mixture and the polymer network (Fig. S2b). All samples prepared for this examination are composed with an excess of acrylate functional groups relative to the thiols. Accordingly, crosslinking in the polymer stabilizing network is primarily associated with acrylate homopolymerization. Both NMR and FTIR measurements confirm near total conversion of the acrylates, similar to prior studies.[20,25]

Upon polymerization, the stabilizing network (depicted in Fig. 1a) retains the chirality of the cholesteric phase (referred to as "structural chirality") in the case of the materials in this manuscript the chirality is left-handed. Thereafter, the low-molar mass liquid crystal preferably aligns to the polymer stabilizing network. Upon application of an DC electric field, ions trapped on or within the polymer stabilizing network facilitate deformation of the structurally chiral polymer network. The deformation results in a concurrent

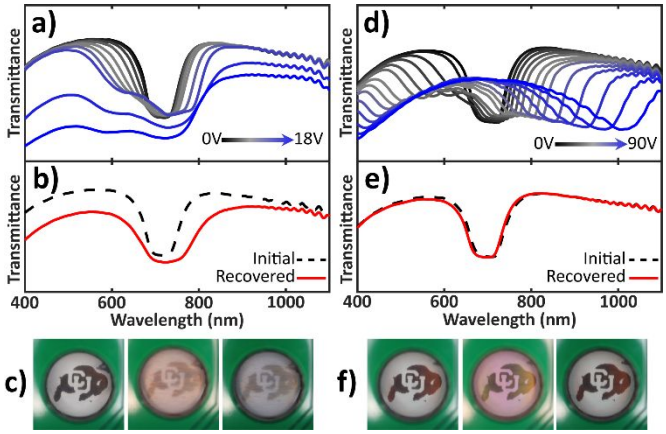

Fig. 2 Representative spectrum and photos for a "poor" performing (a-c) and "good" performing (d-f) sample in this study. These samples were prepared with (a-c) 5wt% RM82, (d-e) 15wt% RM82 with a molar ratio of RM82 to HDT of 2.5:1, each sample also contains 5wt% each of the left-handed chiral dopants, S811 and S1011, 0.5wt% of the radical photoinitiator I-651, in the nematic LC host MLC-2079. (a,d) Spectra of the samples tuning, the voltage range applied to the samples is indicated in the inset. (b,d) Spectra after 10 minutes of recovery at 0V, with a comparison to the initial spectrum prior to voltage application. (c,f) Photos of the PSCLC sample cell in the voltage application holder under diffuse white light with the printed image behind the cell. From left to right the photos show the sample at 0V prior to tuning, at the maximum applied voltage indicated above, and after 10 minutes of recovery.

reconfiguration of the pitch of the anchored, low-molar mass liquid crystal which results in dynamic changes in the optical properties. Here, we are focused on understanding the coupling and interplay of monomer concentration, crosslink density, and retention of structural chirality in compositions that undergo red-shifting tuning of the selective reflection.

The contribution of composition has been subject to prior study, including the overall monomer concentration and inclusion of monofunctional acrylate comonomers.[15,22] No prior study has examined approaches that directly affect the molecular weight between crosslinks in the polymer stabilizing networks. On one hand, it could be expected that "softening" the polymer network would enhance the magnitude of tuning. However, it could also be possible that reducing the crosslink density could distinctly affect the retention of structural chirality and recovery of the material system after application of an electric field.

This potential trade-off is evident in Fig. 2 which compares the electro-optic response and recovery of PSCLC prepared with 5wt% RM82 with a 2.5:1 molar ratio of RM82 to HDT to the response from a sample prepared with 15wt% RM82 with the same ratio of RM82 to HDT. While prior study of monomer concentration has shown comparatively reduced response and recovery as monomer concentration increased,[15] this comparison illustrates that increasing monomer concentration can increase the magnitude of tuning and improve the recovery. The PSCLC prepared with 5wt% RM82 is only able to red-shift λ_c approximately 15nm from the original notch position ($\lambda_{c,o}$). Further increasing the magnitude of the field results in haze in the sample (Fig. 2a). After the field is removed, the sample recovers some degree of the reflection but generally retains scattering character. This is particularly evident in the reduced transmission outside the reflection notch (Fig. 2b). The sample with the same molar ratio of RM82 to HDT but a higher concentration of RM82 is distinct in that it exhibits a high degree of red-shifting, at its farthest point λ_c has shifted approximately 300nm from $\lambda_{c,o}$ (Fig. 2d). In the voltage on state, the reduction in transmission at the wavelengths lower than the original notch position is not due to haziness but rather partial reflection due to the compressed pitches in the sample along with a reduction in transmission from the LC cell. The PSCLC prepared with this concentration exhibits near complete recovery after 10 minutes (Fig. 2e). The influence of composition on retention of optical quality is evident in the photos presented in Fig. 2c,f where the images from left to right show the sample prior to voltage application, during the max voltage application, and after recovery.

These results motivate further study to examine how the association of structural chirality, deformation, electro-optic response, and recovery must balance factors relating to the elastic deformability and toughness (e.g., robustness to deformation) of polymer stabilizing networks. In the case of the PSCLC prepared with 5wt% RM82 (2.5:1 RM82:HDT) it is evident in the limited overall tuning range that the structural chirality is not well maintained in the sample as field strength increases. The increase in haze with applied voltage, given that both the nematic host and polymer stabilizing network have negative dielectric anisotropy, indicate that the polymer stabilizing network is being disrupted out of plane which is then creating optically scattering defects. Microscope images between cross-polarizers show a large increase in defects when the sample starts exhibiting increased haziness, Fig. S3a(I-VII). After the field is removed, the disruption of the polymer stabilizing network is also evident in the poor recoverability, possibly in part due to permanent restructuring or damage to the polymer network. This can be seen in Fig. S3a(VIII) as a permanent increase in the concentration of defects (primarily "oily streaks"). Comparatively, the higher concentration PSCLC is able to deform and recover to the original optical properties. There are no changes to the defects during voltage application or recovery, only a change in the color of transmittance, Fig. S3b(I-VIII).

Prior examinations have largely prepared PSCLCs via the homopolymerization of RM82 (or other diacrylate liquid crystalline monomer). From Figure 2, it is clear that samples prepared with variation in crosslink density may have an optimal composition balancing monomer concentration and crosslink density. This variable space is explored in the data presented in Figure 3(a-d). Here, PSCLCs were prepared at four monomer concentrations (5, 10, 15, and 20 wt% RM82) with molar ratio to HDT ranging from 10:1 (highest crosslink density) to 2.5:1 (lowest crosslink density). All samples prepared red-shifted under voltage application. Control samples prepared without HDT exhibit bandwidth broadening rather than tuning. Prior investigations detail that this can be due to differences in mechanical properties, ion density, or ion affinity. Measurements of the ionic density prior to polymerization were performed and indicated the thiol introduced 10% or less of the total ions in the system with the majority coming from the chiral dopants, RM82, and the photoinitiator (Table S1).[32,33]

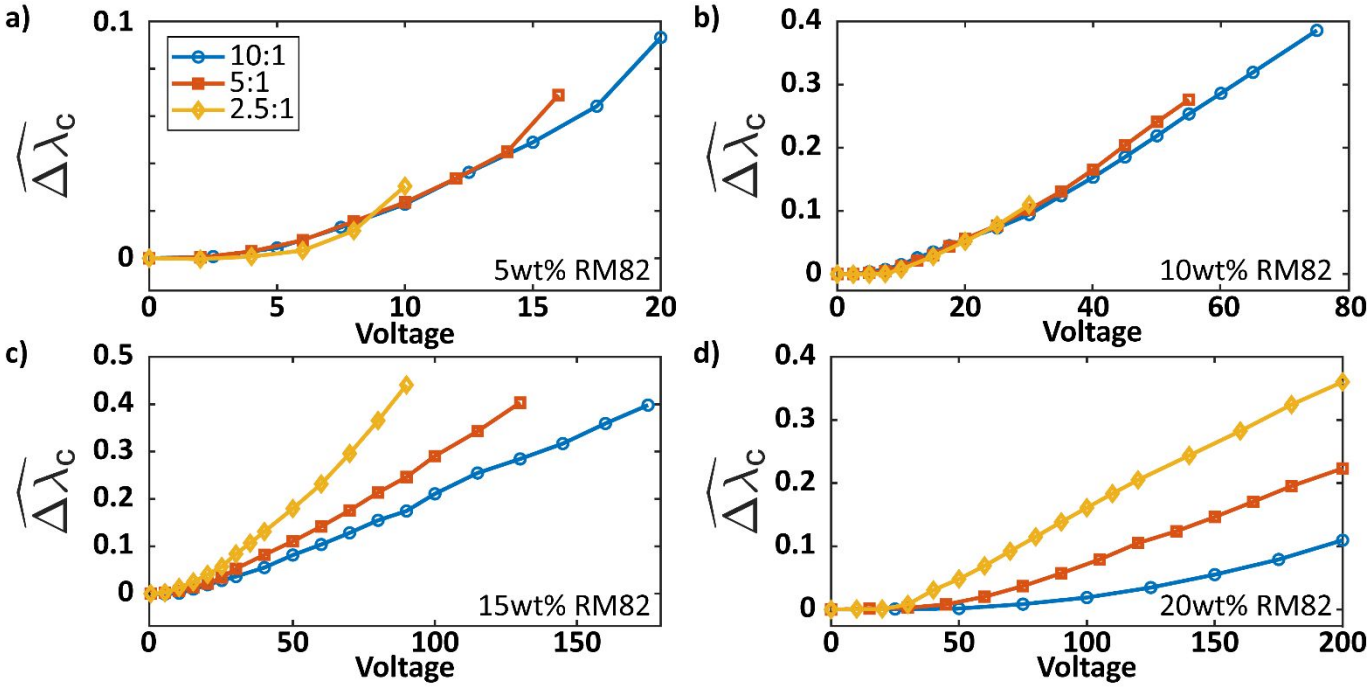

Fig. 3 Change in the tuning factor ($\Delta\lambda_c$) versus voltage for samples prepared with various weight percentages of RM82, the concentration of RM82 present in the mixture is shown in the inset. The legend present in (a) represents the molar ratio of RM82 to HDT, this legend also applies for (b-d). Each sample also contains 5wt% of each chiral dopant, S811 and S1011, 0.5wt% of the radical photoinitiator, I-651, in the nematic LC host MLC-2079.

To simplify discussion we will be utilizing a dimensionless value to compare tuning capabilities which we will call the tuning factor($\widehat{\Delta\lambda_c}$).

$$\widehat{\Delta\lambda_c} = \frac{\lambda_c - \lambda_{c,o}}{\lambda_{c,o}}$$

This value normalizes the tuning for differences in the original notch position. Positive values indicates a red-shifting of λ_c and therefore an increase in the pitch length through the bulk of the sample.[19] For example a tuning factor of 0.1 is equal to 10% increase in the pitch length, so a sample under voltage with $\lambda_{c,o}$ = 700nm will have λ_c = 770nm.

(Fig. 3(a-d) presents the tuning factor versus the voltage applied for the twelve compositions. Data presented are from spectra that retain highly reflective bandgaps absent of degradation (e.g., haze). In some samples, the maximum range of our spectrometer (for these samples that corresponds approximately to $\widehat{\Delta\lambda_c} = 0.4$) was reached or maximum voltage (200V) was applied.

For samples prepared with typical monomer concentrations of 5 or 10wt%, Fig. 3a and 3b respectively, there is relatively little change in the association of tuning and voltage as the crosslink density changes. However, these samples did exhibit significant differences in the maximum achievable tuning range, after which higher applied field results in limited additional tuning, in addition to the samples going hazy, and exhibiting poor recovery (e.g., data in Fig. 2a-c). Increasing the concentration to 15wt% prevented any measurable degradation of the electro-optic response within the confines of our compositional range. In addition, these samples all fully recovered to their initial reflection. It should be noted as a result of using a constant photoinitiator concentration across all sample compositions that the stabilizing networks in samples prepared with the same ratio of RM82 to HDT and different concentrations of RM82 will inherently have different elasto-mechanical properties. The higher the monomer concentration the higher the crosslink density will be, therefore, the networks prepared from higher monomer concentration will be more robust.

In the case of the 5 and 10wt% samples, it is likely that the network is not robust with the addition of HDT which is why unlike the higher concentration samples they have limited tuning, optical degradation, and don't fully recover. In comparison, PSCLCs with monomer concentrations of 15 and 20wt%, which would not have been electro-optically active in a standard formulation (e.g, purely RM82), were all limited by either our systems spectrometer range or maximum voltage. Notably, at these high monomer concentrations, Fig. 3c-d, the samples tuning factor separates significantly as voltage increases. As the thiol concentration increases, softening the network, lower voltages are required for equivalent tuning. The PSCLCs maintained reflectivity as the sample were tuned and also recovered fully.

To further examine the relationship between electro-optic response and crosslink density, we examine coupling of the tuning factor and voltage response (effectively tuning rate) from the data presented in Fig. 3, this analysis is presented in Fig. 4. In this evaluation the higher the value of tuning rate the more sensitive the sample tuning is to voltage. For the lowest weight percent samples, 5wt% RM82 (Fig 4a) a clear pattern is seen, after starting at a low sensitivity above the threshold voltage to begin tuning there is a levelling off of the sensitivity prior to an inversion where the sensitivity rapidly increases. This plateau in sensitivity is seen across the range of monomer concentration and crosslink densities. The highest values and a rapid increase in sensitivity appears to correlate

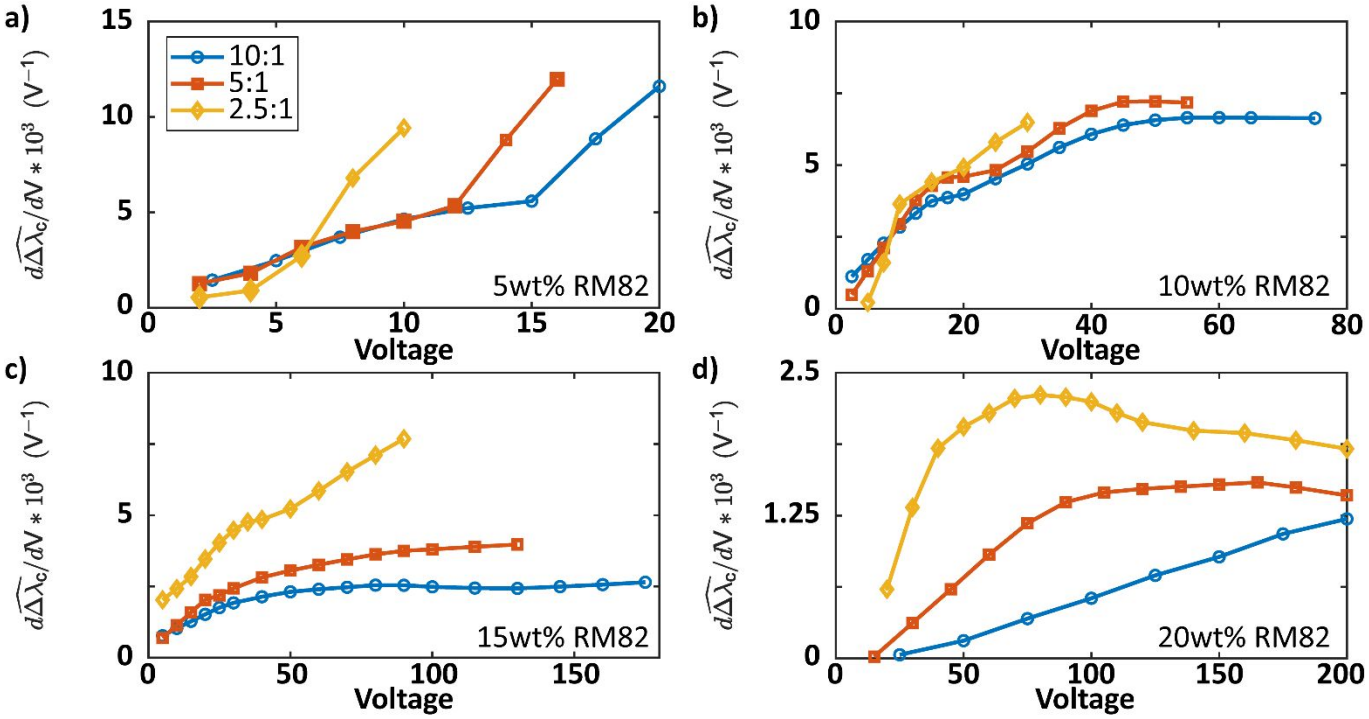

Fig. 4 The tuning rate vs voltage for the data presented in Fig. 3. The initial region near the threshold voltage has been omitted. The values were calculated without fitting or smoothing utilizing the gradient function in MatLab

with approaching a optical degradation and non-recoverability. This implies that the higher weight percentage samples could be tuned significantly higher degree prior to damage if not limited by the voltage application of our system. The range of sensitivity values further suggests that a lower crosslink density, obtained either through HDT addition or monomer concentration, is easier to deform independent of how this affects the network's ability to trap ionic species.

As evident in Fig. 2, the contribution of composition can also considerably affect the recovery of the PSCLCs after field removal. In Fig 5(a) the PSCLC samples were subject to different magnitudes of step changes in the electric fields and their response was monitored. Spectra were collected and analyzed to plot the tuning factor as a function of time to assess the "on" and "off" time switching speeds. Generally, the "on" time is approximately the same for a given change in wavelength. Application of higher strength fields was not performed as the thiol concentration increased because it would have damaged the sample. Voltages were chosen so the samples would achieve approximately the same tuning factor at equilibrium.

The differences in response times are more evident in Fig. 5b when we concentrate on the first voltage pulse. The softening of the polymer network at a constant monomer concentration via the incorporation of HDT has relatively little effect on the tuning dynamics upon voltage application, however the recovery time shows a direct dependence, with the PSCLC based on lower concentration of HDT (e.g., more crosslinked) recovering slower at 14 seconds (10:1 RM82:HDT) compared to 4 seconds for the lower crosslinked sample (2.5:1 RM82:HDT). This pattern continues for the other monomer concentrations (5wt% RM82 has been omitted from this analysis due to the low range of tuning available) and is

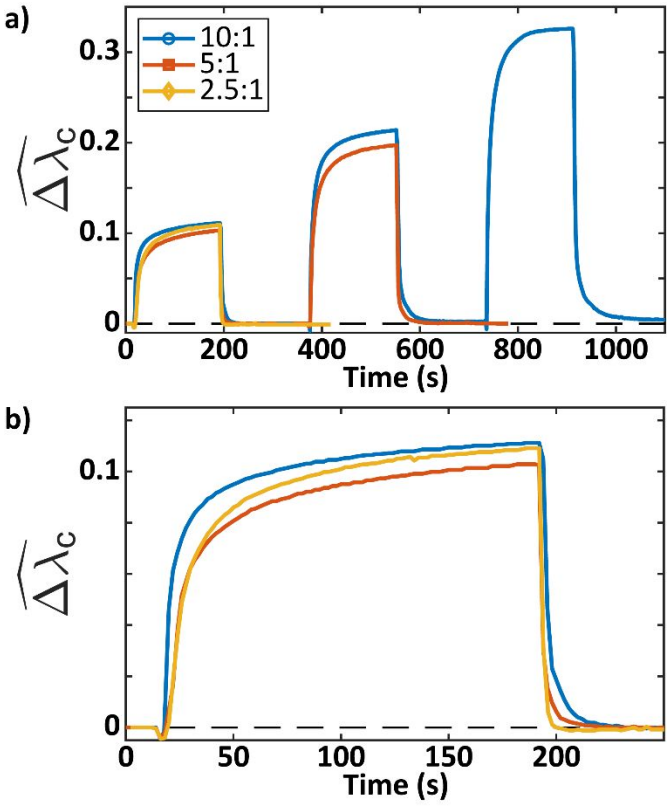

Fig. 5 Dynamic data showing the tuning and recovery of samples prepared with 10wt% RM82 under various voltages, the molar ratio of RM82 to HDT is shown in the legend. The voltages applied were held for 3 minutes and the samples were given 3 minutes to relax at 0V before moving to the next voltage. The following voltages were applied (10:1) 31, 47.2, 62.1, (5:1) 29.6, 44.5, (2.5:1) 28.5. (b) The same data from (a) zoomed in to only the first voltage application and recovery.

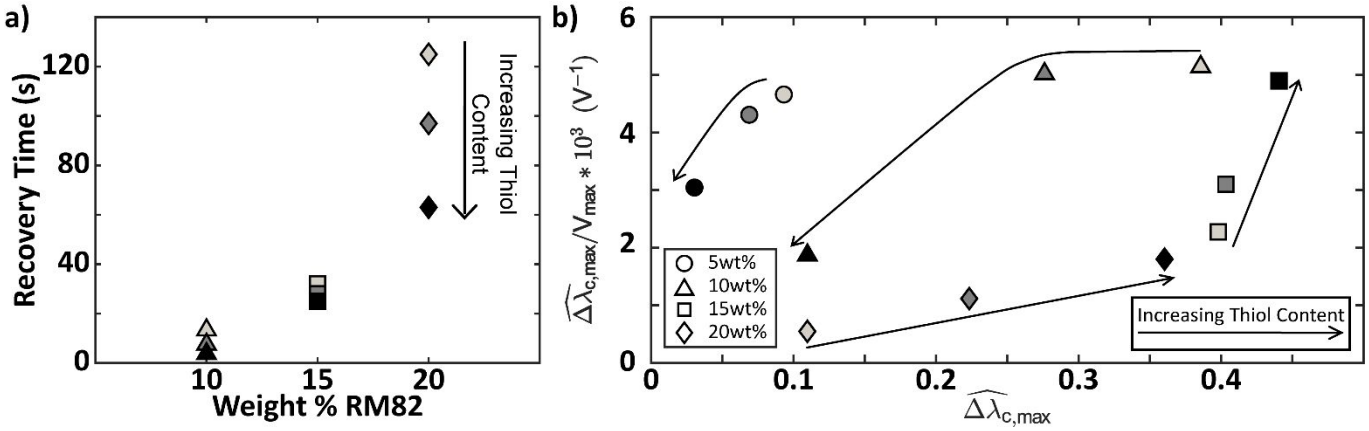

Fig. 6 (a) The recovery time for the samples in this study all tuned the same degree ($\Delta\lambda_c$ = 0.1). The recovery time was evaluated as the time taken to shift from the position when the voltage was turned off to 98% of the recovered equilibrium. Increasing thiol content is indicated by the darkening of the symbol. (b) The maximum tuning factor achieved($\widehat{\Delta\lambda}_{c,max}$) compared to the voltage sensitivity at the same point. The weight percentage of RM82 is designated by the shapes shown in the legend. The color coordinates to the molar ratio of RM82 to HDT, (light gray) 10:1, (dark gray) 5:1, (black) 2.5:1. The arrows follows increasing thiol content for a given weight percentage of RM82.

summarized in Fig. 6a. Based on the decrease in recovery time for decreasing crosslink density independent of monomer concentration as well as the increase in recovery times as the monomer concentration increases the crosslink density, the elasticity of the polymer network can be attributed as the major factor in recovery time.

The interplay between concentration and crosslink density on the electro-optic response and recovery of PSCLCs is further summarized in Fig. 6b. In this plot the farthest the sample tuned is designated as $\widehat{\Delta\lambda}_{c,max}$ and the corresponding voltage for that tuning factor as V_{max}. By dividing $\widehat{\Delta\lambda}_{c,max}$ by V_{max} we obtain a parameter for the tuning efficiency. As the value increases it indicates that a sample's tuning capabilities are more sensitive to voltage application. A higher value would be more desirable as it would require lower power requirements for a device. This tuning efficiency value is plotted versus the maximum tuning factor. This plot represents efficiency as a variable of tuning capability. The samples with the best overall performance will be located in the upper right area of Fig. 6b, this indicates a high degree of voltage sensitivity and high degree of tunability. In this plot it is easy to see that the HDT inclusion is not always beneficial. For samples made with either 5 or 10wt% RM82 the sensitivity and tunability of the sample is harmed by the softening of the network. While the samples prepared with 15 and 20wt% RM82 the sensitivity and the tunability are both improved.

Conclusions

The electro-optic response of PSCLCs were investigated in samples in which the crosslink density of the polymer stabilizing network was adjusted by the inclusion of a difunctional thiol monomer which was incorporated into the acrylate polymer network through photo-initiated radical polymerization. The influence of the dithiol on crosslink density within the PSCLC devices had a significant impact on the electro-optic response. An optimal concentration was identified. Notably, the recovery of the optical reconfiguration was directly correlated to the elasticity of the polymer stabilizing network affected by HDT addition. With an improved measurement system the design space explored in Fig. 6b could be expanded allowing for a wider range of compositional study.

Methods

Sample Preparation

Mixtures were prepared with the dielectric nematic liquid crystal host MLC-2079 (Merck, Δε = -6.1, Δn = 0.15), 1,6-Hexanedithiol (Sigma), RM82 (Willshire Technologies), left-handed chiral dopants S811 and S1011 (Merck), and the photoinitiator 2,2-dimethoxy-2-phenylacetophenone (I-651, iGM Resins). These compounds were melt mixed in the isotropic phase with a vortex mixer and a heat gun at 130°C. The mixtures were capillary filled into glass cells on a hot plate at 50°C and held at that temperature for 5 minutes before slowly cooling to room temperature. The glass cells were obtained from Instec Inc. (S type, 1cm² active ITO area (100Ω/sq), 20 µm cell gap, planar alignment layer with anti-parallel rubbing angles). After cooling the samples were polymerized at room temperature under a UV Flood Lamp (365nm, 50mW/cm², 10min) (Dymax-RediCure).

Electro-optic Measurements

Transmission spectra were taken with STS-VIS and STS-NIR spectrometers (Ocean Insight) concurrently with an unpolarized beam provided by a halogen bulb light source. Spectra was captured with the Ocean View software while a DC field was applied via the Instec LCH–S 11 cell holder. Spectral analysis was performed automatically by a custom programmed MatLab script developed internally.

NMR Measurements

NMR spectra were collected on a Bruker Avance-III 400MHz NMR at room temperature in DMSO-D6. Monomer components were measured as pure components dissolved in DMSO-D6. For analysis a nematic liquid crystal (NLC) model system consisting of 20wt% RM82,

a 2.5:1 molar ratio of RM82 to HDT, and 0.5wt% I-651 in MLC-2079 was employed. The NLC mixture was measured after mixing. After polymerization the glass cell was cracked open and the polymer stabilized mixture removed and mixed into a dry vial with DMSO-D6. After 24 hours at room temperature the liquid was decanted off leaving the polymer network behind, this solution was then measured.

FTIR Measurements

FTIR spectra were collected on an ATR accessory of a Thermo-Scientific Nicolet iS50 spectrometer with liquid nitrogen cooled MCT-A detector. The NLC mixture used in the NMR measurements was also measured. The polymer network was measured by polymerizing the mixture then soaking the cell in hexanes for 3 days to extract the non-reacted components. After removing the cell and allowing the solvent to evaporate over 48 hours the cell was cracked open. The polymer network was collected and measured.

Optical Imaging

Photomicrographs were obtained on a Nikon Eclipse Ci-Pol polarized optical microscope with . Voltage was applied via the Instec cell holder.

Ion Density Measurements

The LC cell placed in the Instec cell holder was inserted into a grounded Faraday shield. A square wave voltage (5V, 0.1Hz) was applied by an NI USB-6001 DAQ. The current was measured by a Keithley 6485 picoammeter with a 200nA threshold and transmitted to the NI DAQ for recording at a sample rate of 4000 samples per second. The ionic density was calculated by the transient leakage current measurement method described by Colpaert et al.[32]

Conflicts of Interest

The authors have no conflicts to declare.

Acknowledgements

This work was made possible by support from the Air Force Office of Scientific Research (AFOSR) (B.P.R., G.K.P, T.J.W.). B.P.R. also acknowledges partial fellowship support via the Graduate Assistance in Areas of National Need (GAANN) fellowship through the Department of Education (DOE).

References

1 H.-S. Kitzerow and C. Bahr, Eds., *Chirality in Liquid Crystals*, Springer, 2001.
2 I. Dierking, *Polymer Modified Liquid Crystals*, Royal Society of Chemistry, London, 2019.
3 S.-T. Wu and D. Yang, *Reflective Liquid Crystal Displays*, Wiley, 2001.
4 H.-G. Kuball and T. Hofer, in *Chirality in Liquid Crystals*, eds. H. Kitzerow and C. Bahr, Springer-Verlag New York, 1st edn., 2001, pp. 67–100.
5 G. Chilaya, in *Chirality in Liquid Crystals*, eds. H. Kitzerow and C. Bahr, Springer-Verlag New York, 1st edn., 2001, pp. 159–185.
6 P. Yeh and C. Gu, *Optics of Liquid Crystal Displays, 2nd Edition*, Wiley, 2010.
7 F. Castles and S. M. Morris, in *Handbook of Liquid Crystals*, eds. J. W. Goodby, P. J. Collings, T. Kato, C. Tschierske, H. Gleeson and P. Raynes, Wiley-VCH Verlag GmbH & Co. KGaA, Weinheim, Germany, 2014, vol. 3, pp. 1–28.
8 I. Dierking, *Advanced Materials*, 2000, **12**, 167–181.
9 D. -K. Yang, L. -C. Chien and J. W. Doane, *Appl Phys Lett*, 1992, **60**, 3102–3104.
10 I. Dierking, *Polym Chem*, 2010, 1, 1153–1159.
11 Y. K. Fung, D.-K. Yang, S. Ying, L.-C. Chien, S. Zumer and J. W. Doane, *Liq Cryst*, 1995, **19**, 797–801.
12 B. P. Radka, K. M. Lee, N. P. Godman and T. J. White, *Soft Matter*, 2022, **18**, 3013.
13 D.-K. Yang, Y. Cui and H. Nemati, *J. Appl. Phys*, 2013, **114**, 243515.
14 R. A. M. Hikmet, *Liq Cryst*, 1991, **9**, 405–416.
15 V. T. Tondiglia, L. V. Natarajan, C. A. Bailey, M. M. Duning, R. L. Sutherland, D. Ke-Yang, A. Voevodin, T. J. White and T. J. Bunning, *J Appl Phys*, 2011, **110**, 053109.
16 K. M. Lee, V. P. Tondiglia, M. E. McConney, L. V. Natarajan, T. J. Bunning and T. J. White, *ACS Photonics*, 2014, **1**, 1033–1041.
17 H. Nemati, S. Liu, R. S. Zola, V. P. Tondiglia, K. M. Lee, T. White, T. Bunning and D. K. Yang, *Soft Matter*, 2015, **11**, 1208–1213.
18 M. E. Mcconney, V. P. Tondiglia, L. V. Natarajan, K. M. Lee, T. J. White and T. J. Bunning, *Adv Opt Mater*, 2013, **1**, 417–421.
19 K. M. Lee, V. P. Tondiglia, T. Lee, I. I. Smalyukh and T. J. White, *J Mater Chem C Mater*, 2015, **3**, 8788–8793.
20 K. M. Lee, V. P. Tondiglia, N. P. Godman, C. M. Middleton and T. J. White, *Soft Matter*, 2017, **13**, 5842–5848.
21 K. M. Lee, V. P. Tondiglia and T. J. White, *ACS Omega*, 2018, **3**, 4453–4457.
22 B. P. Radka, B. E. King, M. E. McConney and T. J. White, *Adv Opt Mater*, 2020, **8**, 2000914.
23 V. P. Tondiglia, L. V. Natarajan, C. A. Bailey, M. E. McConney, K. M. Lee, T. J. Bunning, R. Zola, H. Nemati, D.-K. Yang and T. J. White, *Opt Mater Express*, 2014, **4**, 1465.
24 K. M. Lee, E. P. Crenshaw, M. Rumi, T. J. White, T. J. Bunning and M. E. McConney, *Materials*, 2020, **13**, 746.
25 K. M. Lee, T. J. Bunning, T. J. White, M. E. McConney and N. P. Godman, *Crystals (Basel)*, 2021, **11**, 1–10.
26 K. A. Berchtold, B. Hacioglu, L. Lovell, J. Nie and C. N. Bowman, *Macromolecules*, 2001, **34**, 5103–5111.
27 K. A. Berchtold, L. G. Lovell, J. Nie, B. Haciolu and C. N. Bowman, *Polymer (Guildf)*, 2001, **42**, 4925–4929.
28 L. G. Lovell and C. N. Bowman, *Polymer (Guildf)*, 2003, **44**, 39–47.

29 T. H. Ware, Z. P. Perry, C. M. Middleton, S. T. Iacono and T. J. White, *ACS Macro Lett*, 2015, **4**, 942–946.

30 T. S. Hebner, H. E. Fowler, K. M. Herbert, N. P. Skillin, C. N. Bowman and T. J. White, *Macromolecules*, 2021, **54**, 11074–11082.

31 N. B. Cramer and C. N. Bowman, *J Polym Sci A Polym Chem*, 2001, **39**, 3311–3319.

32 C. Colpaert, B. Maximus and A. De Meyere, *Liq Cryst*, 1996, **21**, 133–142.

33 Y. Garbovskiy, *Proceedings 2020, Vol. 62, Page 10*, 2021, **62**, 10.